Roughness effect on heterojunction photovoltaics

Palasantzas, Georgios; Koumanakos, E.

Published in:
Journal of Applied Physics

DOI:
10.1063/1.362532

Publication date:
1996

Roughness effect on heterojunction photovoltaics

G. Palasantzas and E. Koumanakos
G. S. A. Research and Development Center, Amygdaleza-Aharnes, 13600 Athens, Greece

(Received 11 December 1995; accepted for publication 29 February 1996)

In this work, we present an investigation of the junction interface roughness effect on the open circuit voltage, V_{oc} for thin film heterojunction photovoltaics. The roughness effect is studied for self-affine rough interfaces, which are described in Fourier space by the correlation model $\sim\sigma^2\xi^2(1+aq^2\xi^2)^{-1-H}$. σ, ξ, and H denote, respectively, the rms roughness, the in-plane roughness correlation length, and the interface irregularity exponent ($0<H<1$). The roughness effect becomes significant for small H (<0.5), and for large long-wavelength roughness of typical values $\sigma/\xi\sim0.1$. The junction interface roughness may yield a contribution to V_{oc} even up to 10%. Comparison of the results is performed with predictions in real heterojunctions, e.g., Cu_xS/(Zn)CdS. © *1996 American Institute of Physics.* [S0021-8979(96)05211-5]

I. INTRODUCTION

Among the various energy sources which involve control of natural phenomena, solar energy is possibly considered the most attractive. This is due to the fact that this energy source is costless, renewable, and abundant. Conversion of solar to electric energy is based on the photovoltaic (PV) phenomenon.[1] Even from the time they were first developed in the 1950s to provide electrical power for spacecrafts,[2] PV elements have been touted as an energy source with a bright technological future.[3]

Despite the enormous efforts up to now, PV cells have been less than a shining success. The basic reason is the high production cost which limits their use to niche applications such as powering watches and calculators or providing electricity in remote homes beyond the reach of power lines. PV elements are generally constructed from semiconductor $p-n$ homojunctions (i.e., Si), and heterojunctions [i.e, Cu_xS/(Zn)CdS, CdS/CdTe, $Al_xGa_{1-x}As$, CdS/Cu_2SnS_3, $CuInSe_2$, ITO/CdTe, In/CdTe, etc.],[5] as well as organic systems (i.e., C_{60} polymers).[4]

Crystalline Si, which provides the most reliable solar cells, is produced by a costly precision process akin to manufacturing computer chips, and organic solar cells have stability problems when exposed to strong light and short lifetimes.[4] Alternatively, thin film heterojunctions for PV elements[5] can be produced from elements abundant in nature with significant efficiency and having a large junction area. If we denote by A_x and A_{flat} the junction area and the illuminated area of the PV element, the ratio A_x/A_{flat} can drastically affect the element's characteristics. Moreover, this ratio is not directly related to principal properties of the semiconductors. It is related to the method and the film fabrication conditions, which can significantly affect the PV element's efficiency.

In many instances, the fabrication of the thin film heterojunction includes vapor deposition and sputtering (i.e., Cu_xS/CdS, CdS/CdTe, etc.), which are in general nonequilibrium processes. The formation of surfaces/interfaces with self-affine fractal morphology is observed in many cases for vapor deposited and/or sputtered films under conditions far from equilibrium.[6] Although interface roughness has been well studied in resonant tunneling diodes, a thorough study of the interface junction roughness effect on PV devices is still in its infancy. Therefore in this work, we will investigate the effect of random roughness interface morphology on the open circuit voltage (V_{oc}). It is expected that the presence of junction interface roughness will degrade the electrical properties (lower V_{oc} in the present case) of the PV element. Also, our results will be compared with experimental data.

II. BASIC PV-ELEMENT THEORY

The photovoltage is created by the dissociation of electron–hole pairs due to incident photons within the junction built-in field. The energy gap E_{gap} of the photon absorber should be adjusted to the energy of the incident photons. In fact, large energy gaps result in a small number of generated charged pairs and thus small photocurrent, while small energy gaps result in a small open circuit voltage. It is estimated that a favorable energy gap for the photon absorber must be in the range 1 eV$<E_{gap}<$1.7 eV.[5,7]

The current–voltage ($I-V$) relation for a PV element is given by[2,5]

$$I=A_xJ_0[e^{q(V-IR_s)/kT}-1]-A_{flat}J_{ph}h(V), \tag{2.1}$$

where $h(V)$ is the collection factor of the $p-n$ junction. A_x the junction area, A_{flat} the illuminated area, R_s the resistance in series, J_{ph} the photocurrent density, J_0 the saturation current at inverse polarization, T the system temperature, k the Boltzman constant, and q the carrier charge.

The open circuit voltage V_{oc} is obtained from Eq. (2.1) by setting $I=0$. Thus, we have

$$\begin{aligned} qV_{oc}&\approx kT\ \ln\left[\frac{J_{ph}h(V_{oc})}{J_0}\right]+(qV_{oc})_r,\\ (qV_{oc})_r&=-kT\ \ln\left[\frac{A_x}{A_{flat}}\right]\end{aligned} \tag{2.2}$$

because in general $e^{qV/kT}\gg1$. This can readily be seen from the fact that at $T\sim300$ K we have $kT\sim0.028$ eV and since $qV\sim0.1$–1 eV, we obtain $e^{qV/kT}\gg1$. The first term in Eq. (2.2) is positive, while the second term $(V_{oc})_r$, which is mainly related to the heterojunction fabrication conditions, is negative since $A_x\geqslant A_{flat}$.

III. AREA OF A ROUGH SURFACE

If we denote the surface height profile by $h(r)$, which is assumed to be a single-valued function of the in-plane position vector $r=(x,y)$, the area of a rough interface is given by

$$A_x=\int [1+(\nabla h)^2]^{1/2}d^2r. \tag{3.1}$$

For weak roughness $|\nabla h|\ll 1$, $[1+(\nabla h)^2]^{1/2}\approx 1+(1/2)(\nabla h)^2-(1/8)(\nabla h)^4,...,$ which upon substitution into Eq. (3.1) yields up to second order

$$A_x\approx A_{\text{flat}}+\frac{1}{2}\int (\nabla h)^2 d^2r-\frac{1}{8}\int (\nabla h)^4 d^2r, \tag{3.2}$$

where the average flat area is given by $A_{\text{flat}}\approx\int d^2r$. In the strong roughness limit or $|\nabla h|\gg 1$, $[1+(\nabla h)^2]^{1/2}\approx|\nabla h|+(1/2)|\nabla h|^{-1}$, substitution into Eq. (3.1) yields

$$A_x\approx\int |\nabla h| d^2r+\frac{1}{2}\int |\nabla h|^{-1} d^2r. \tag{3.3}$$

IV. THEORY FOR RANDOM ROUGHNESS AND SELF-AFFINE ROUGHNESS

The surface height profile $h(r)$ is assumed to be a stationary stochastic process with $\langle h(r)\rangle=0$, and the surface isotropic along the x and y axes. The angular brackets denote an average over the ensemble realizations of the surface profile, $\sigma^2=\langle h(r)^2\rangle$ is the mean-square departure of the surface from flatness (rms surface roughness), and ξ the in-plane roughness correlation length which represents the average distance between consecutive peaks or valleys on the surface. In addition, we shall assume $h(r)$ to be a random Gaussian variable in order to calculate ensemble averaged products of $h(r)$'s (see the Appendix).

We will define the Fourier transform of $h(r)$, and the correlation function $C(r)$ by

$$\begin{aligned} h(q)&=\frac{1}{(2\pi)^2}\int h(r)e^{-iqr}d^2r,\\ C(r)&=\frac{1}{A_{\text{flat}}}\int \langle h(r+r')h(r')\rangle d^2r' \end{aligned} \tag{4.1}$$

which in turn yield $\langle h(q)\rangle=0$ since $\langle h(r)\rangle=0$, and

$$\begin{aligned} \langle|h(q)|^2\rangle&=\frac{A_{\text{flat}}}{(2\pi)^4}\int C(r)e^{-iqr}d^2r,\\ \langle h(q)h(q')\rangle&=\frac{(2\pi)^4}{A_{\text{flat}}}\langle|h(q)|^2\rangle\delta^2(q-q'). \end{aligned} \tag{4.2}$$

The right-hand side of Eq. (4.2), which gives the averaged products $\langle h(q)h(q')\rangle$, means that the surface is assumed to be statistically stationary up to second order or translationally invariant.

A wide variety of surfaces and interfaces occurring in nature are well represented by a kind of roughness associated with self-affine fractal scaling, defined by Mandelbrot in terms of fractional Brownian motion.[8] Examples include the nanometer topology of vapor-deposited films, the spatial fluctuations of liquid–gas interfaces, the kilometer-scale structure of mountain terrain, etc.[6,8] Physical processes which produce such surfaces include fracture, erosion, molecular beam epitaxy, fluid invasion in porous media, etc.[6,8]

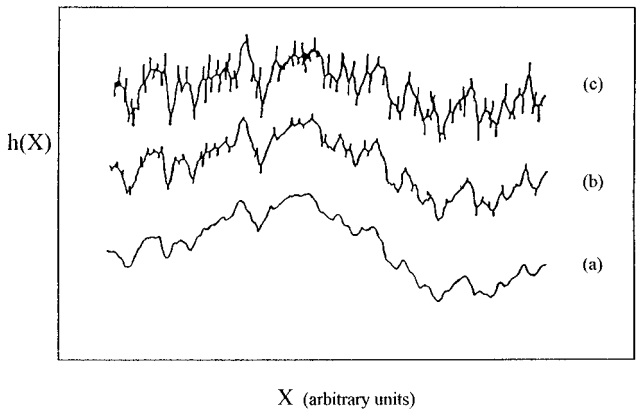

FIG. 1. Schematics of the height profile $h(X)$ vs the in-plane position X for self-affine structures in order to show the effect of the roughness exponent H (see Refs. 6 and 8): (a) $H=0.8$, (b) $H=0.5$, (c) $H=0.2$.

The correlation function for any physical self-affine surface is characterized by a finite correlation length ξ, which is a measure of the average distance between peaks and valleys on the surface such that $C(r)\approx\sigma^2-Dr^{2H}$ for $r\ll\xi$, and $C(r)=0$ for $r\gg\xi$ ($D\sim\sigma^2/\xi^{2H}$ is a constant).[8–11] The roughness exponent $0<H<1$ is a measure of the degree of surface irregularity.[8,10] Small values of $H(\sim 0)$ characterize extremely jagged or irregular surfaces, while large values characterize $H(\sim 1)$ surfaces with smooth hills and valleys, Fig. (1).[10,11]

The Fourier transform $\langle|h(q)|^2\rangle$ of $C(r)$ according to Eq. (4.1) for self-affine fractals, has the scaling behavior $\langle|h(q)|^2\rangle\propto q^{-2-2H}$ if $q\xi\gg 1$, and $\langle|h(q)|^2\rangle\propto$const if $q\xi\ll 1$.[8] This scaling behavior Fourier space for self-affine structures is satisfied by the k-correlation model.[11] This model is valid for the whole range of values for the roughness exponent $0\leqslant H<1$, and following the notation of Ref. 11, $\langle|h(q)|^2\rangle$ is given by

$$\langle|h(q)|^2\rangle=\frac{A_{\text{flat}}}{(2\pi)^5}\frac{\sigma^2\xi^2}{(1+aq^2\xi^2)^{1+H}}, \tag{4.3}$$

where the normalization condition $[(2\pi)^4/A]\times\int_{0<q<Q_k}\langle|h(q)|^2\rangle d^2q=\sigma^2$ yields the parameter ''a'': $a=1/2H[1-(1+aQ_c^2\xi^2)^{-H}]$, $(0<H<1)$ and $a=1/2\ \ln(1+aQ_c^2\xi^2)$ $(H=0)$. Expressions valid for $H=0$ can be obtained from those valid for $H>0$, if we consider the identity $\lim_{H\to 0}(1/H)[x^H-1]=\ln(x)$. The limiting case of logarithmic roughness $(H=0)$ is related to predictions of various growth models for the nonequilibrium analog[12] of the equilibrium roughening transition.[13] In addition, the knowledge of the following integral will be useful in calculations of the surface area (also see the Appendix), which is calculated analytically in terms of Eq. (4.3),

$$S_r(\sigma,\xi,H)=\frac{(2\pi)^4}{A_{\text{flat}}}\int q^2\langle|h(q)|^2\rangle d^2q$$
$$=\frac{\sigma^2}{2a^2\xi^2}\left\{\frac{1}{1-H}[(1+aQ_c^2\xi^2)^{1-H}-1]-2a\right\}. \tag{4.4}$$

V. RESULTS AND DISCUSSION

Weak roughness limit: Fourier transformation of Eq. (3.2) in combination with Eqs. (A3) and (A4), yields up to second order of perturbation theory

$$\frac{A_x}{A_{\text{flat}}}\approx 1+\tfrac{1}{2}S_r(\sigma,\xi,H)-\tfrac{3}{8}[S_r(\sigma,\xi,H)]^2 \tag{5.1}$$

by proper Fourier transformation of the terms $(\nabla h)^{2n}$ ($n=1,2$) in Eq. (3.2), and grouping of integrated ensemble-averaged products with the $2n$ terms (see the Appendix).

Strong roughness limit: In this case we can calculate mainly an upper limit for the rough area. In fact, the inequality $\langle|\nabla h|\rangle\leqslant\langle|\nabla h|^2\rangle^{1/2}$ yields, after substitution in Eq. (3.3) to lowest order,

$$\frac{A_x}{A_{\text{flat}}}\approx\int\langle|\nabla h|\rangle d^2r\leqslant\int[\langle|\nabla h|^2\rangle]^{1/2}d^2r. \tag{5.2}$$

Fourier transformation of Eq. (5.2) and taking into account Eq. (4.4) yields

$$\frac{A_x}{A_{\text{flat}}}\leqslant[S_r(\sigma,\xi,H)]^{1/2}$$
$$=\frac{\sigma}{\sqrt{2}a\xi}\left\{\frac{1}{1-H}[(1+aQ_c^2\xi^2)^{1-H}-1]-2a\right\}^{1/2}. \tag{5.3}$$

Thus, Eq. (5.3) yields an upper bound for the roughness contribution to first order of approximation.

Prior to the presentation of the results, we point out the following. The ratio σ/ξ describes mainly the long-wavelength ($q\ll 1/\xi$) roughness characteristics. Finer roughness details at short wavelengths ($q\gg 1/\xi$) are revealed through the effect of the roughness exponent H. The latter describes the degree of height–height fluctuation irregularity and density, and it is related with a local interface/surface fractal dimension $D=3-H$.[8] In our calculations, we used, for the correlation length ξ, the fixed value $\xi=40.0$ nm, and values for the rms roughness σ such that $\sigma/\xi\leqslant 0.1$. The values of the roughness exponent H are considered in the range $0\leqslant H<1$. The chosen values for the parameters σ, ξ, and H come from experimental roughness studies over a wide variety of surface systems.[6,9] Finally, we will assume PV elements at room temperature, $T\sim 300$ K, which result in $kT\sim 0.028$ eV.

In Fig. 2, we present schematics of the upper bound given by Eq. (5.3) as a function of the roughness exponent H, and for values of the ratio σ/ξ in the range $0.01<\sigma/\xi<0.1$. It is observed that the upper bound of the rough surface area could be as large as ten times the average flat area (strong roughness limit or $S_r>1$). This occurs mainly at large ratios $\sigma/\xi\sim 0.1$, and small roughness exponents H. The latter is in agreement with the fact that as H becomes smaller ($H<0.5$), the number of surface crevices increases (see Fig. 1), therefore exposing a larger area. Comparisons with real systems reveal that the values for the rough area upper bound can be realistic, since they produce deviations between theory and experiment as we will see later on. Moreover, from Fig. 2 we can see that the dominant effect comes from the ratio σ/ξ. In fact from Eqs. (4.4) and (5.3), the upper bound for the rough area is directly proportional to σ/ξ; $A_x/A_{\text{flat}}\propto\sigma/\xi$. Nevertheless, the increment at small H (<0.5) appears to be characteristically steep as a function of H.

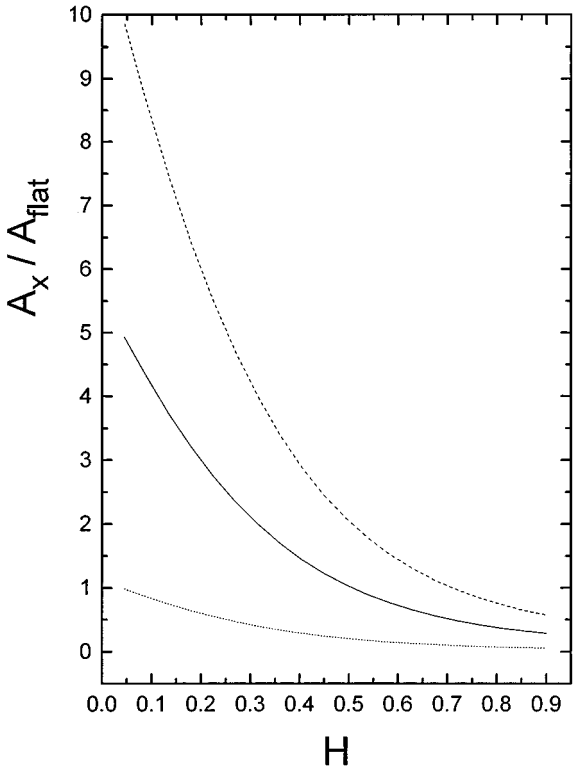

FIG. 2. Schematics of the upper bound for A_x/A_{flat} vs the roughness exponent H in terms of Eq. (5.3): dots $\sigma/\xi=0.03$, solid line $\sigma/\xi=0.05$, and dashes $\sigma/\xi=0.07$. The fixed value for the correlation length $\xi=40$ nm was used during the calculations.

In Figs. 3(a)–3(c), we plot simultaneously the weak roughness limit effect [Eq. (5.1)][ ]with the upper bound strong roughness limit [Eq. (5.3)][ ]as a function of H, and ratios σ/ξ of 0.03, 0.05 and 0.07. In all the schematics, there is a discontinuity in $(V_{\text{oc}})_r$ as function of H which signifies the crossover from the strong to weak roughness limit regime. Furthermore, $(V_{\text{oc}})_r$ in the strong roughness limit is the regime to the order of $\sim 10^{-2}10^{-3}$ V, while $(V_{\text{oc}})_r$ in the weak roughness limit is in the regime of mV and lower ($\sim 10^{-3}$–10^{-4} V). From the same schematics, we observe that as the ratio σ/ξ increases the crossover occurs at larger roughness exponents H. More precisely, we obtain for $\sigma/\xi=0.03$ a crossover at $H\sim 0.4$ for $\sigma/\xi=0.05$ at $H\sim 0.55$, and for $\sigma/\xi=0.07$ at $H\sim 0.65$.

In order to judge the significance of the roughness effect on V_{oc}, comparisons with theoretical and experimental pre-

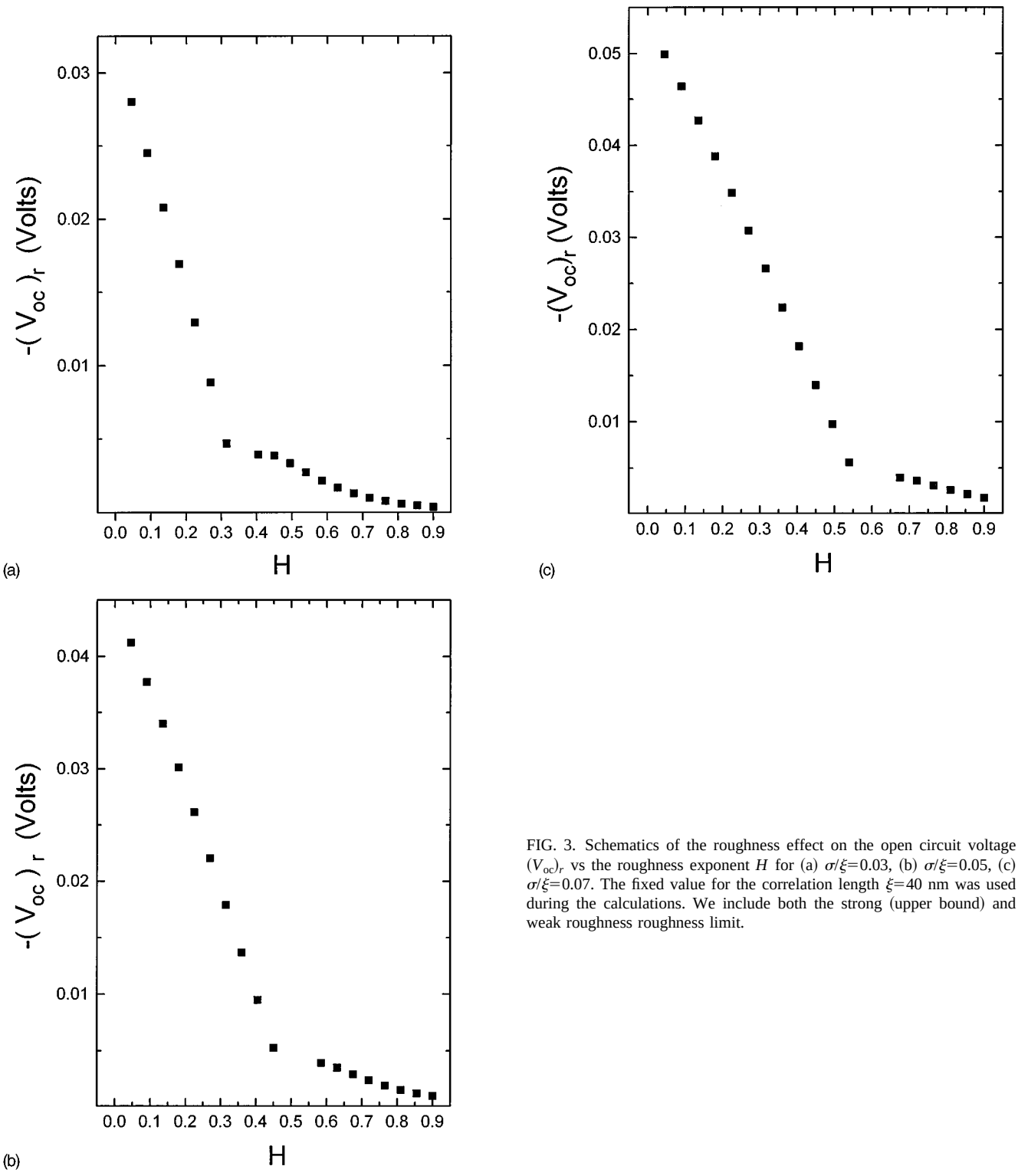

FIG. 3. Schematics of the roughness effect on the open circuit voltage $(V_{oc})_r$ vs the roughness exponent H for (a) $\sigma/\xi=0.03$, (b) $\sigma/\xi=0.05$, (c) $\sigma/\xi=0.07$. The fixed value for the correlation length $\xi=40$ nm was used during the calculations. We include both the strong (upper bound) and weak roughness roughness limit.

dictions on real heterojunction systems should be performed. In measurements of V_{oc}, e.g., in CuxS/ZnCdS films,[5] the measured voltage values were $V_{oc}\sim 0.65-0.71$ V. Nonetheless, a theoretical value was predicted to be $V_{oc}\sim 0.74$ V. On the other hand, as can be seen from Fig. 3 such a difference between theory and experiment is of the order of $(V_{oc})_r$ (roughness contribution) at small roughness exponents $H<0.5$, and typically large ratios σ/ξ (~ 0.1). In Cu_xS/CdS films, with a different fabrication process of Cu_xS, where the latter would not enter too deeply inside the crystallites of CdS, it is possible to yield an improvement of V_{oc} even of ~ 0.06 V (Aperathitis), which is about 10% of V_{oc}.[5] Such a contribution from roughness is closely attained during our calculations in the regime of strong roughness [see Figs. 3(a)–3(c) for $H<0.3$] Thus, the roughness effect can be responsible for significant deviations from expected theoretical

predictions. Furthermore, our calculations can have a close connection with reality, and can be the basis for direct quantitative analysis of junction interface roughness effects in thin film heterojunction PV.

Moreover, it should be pointed out that during the operation of a PV element, heating effects of the thin film can change the junction interface morphology by reducing H and σ/ξ (smoothening effects), which in turn can affect the element's performance. For example, the temperature effect on V_{oc} has been examined for In/CdTe junctions prepared by evaporation of In onto sputter-etched surfaces of CdTe. A decrease of V_{oc} in the range $\sim$1.0–0.4 V for temperatures in the range of $\sim$50–300 K was observed (Courreges *et al.*).[5]

VI. CONCLUSIONS

In conclusion, we combined knowledge of basic PV theory with that of analytic height–height correlation models for self-affine fractals, in order to investigate quantitatively the heterojunction interface roughness effect on the open circuit voltage (V_{oc}). Our results show clearly that this effect becomes of significant quantitative importance even to the order of $\sim 10^{-2}$ V for surfaces with large ratios $\sigma/\xi(\sim 0.1)$, and small roughness exponents $H(<0.5)$ (strong roughness limit). Comparisons with simple experimental systems show the relevance of our calculations with reality. More precisely, our estimations of the strong roughness limit are closer to the presented experimental data where the corresponding rough area is $A_{oc}\sim(9–10)\,A_{flat}$.

Extensive studies will be required on each particular thin-film structure to gauge precisely the junction-roughness effect in connection with film fabrication conditions and system temperature. Moreover in heterojunctions, problems related to lattice mismatch can contribute significantly to the element's efficiency. This is due to the fact that lattice mismatch affects the recombination of the charged pairs prior to their collection, and as a result their investigation remains of crucial technological importance in the solar cell industry.

ACKNOWLEDGMENTS

G.P. would like to acknowledge the hospitality of the G.S.A. Research and Development Center, useful discussions with P. Statiris, A. Moustakas, and correspondence with I. Zagos and B. Friligos. Especially, we would like to thank P. Statiris for critical reading of the manuscript.

APPENDIX

The assumption that $h(r)$ is a Gaussian variable means that the average of any odd number of factors of $h(r)$ with the same or different arguments vanishes, whereas the average of the product of an even number of factors of $h(r)$ is given by the sum of the products of the averages of $h(r)$'s paired two-by-two in all possible ways, i.e., we have[14]

$$\langle h(r)h(r')h(r'')h(r''')\rangle = \langle h(r)h(r')\rangle\langle h(r'')h(''')\rangle + \langle h(r)h(r'')\rangle\langle h(r')h(r''')\rangle + \langle h(r)h(r'''')\rangle\langle h(r')h(r'')\rangle. \quad \text{(A1)}$$

In fact, each pair of $h(r)$'s on the right-hand side of Eq. (A1) is called a contraction. Moreover, Fourier transformation of Eq. (A.1) yields

$$\langle h(q)h(q')h(q'')h(q''')\rangle = \langle h(q)h(q')\rangle\langle h(q'')h(q''')\rangle + \langle h(q)h(q'')\rangle \times\langle h(q')h(q''')\rangle + \langle h(q)h(q''')\rangle\langle h(q')h(q'')\rangle, \quad \text{(A2)}$$

where each pair in Eq. (A2) can be calculated according to Eqs. (4.1), (4.2), and (4.3).

In Eq. (3.2) after ensemble average and substitutions of the Fourier transforms for $h(r)$, integrals of the form

$$\langle(\nabla h)^{2n}\rangle = i^{2n}\int \left\langle \prod_{j=1}^{2n} h(q_j)\right\rangle \times\prod_{j=1}^{2n} q_j \exp\left[-i\left(\sum_{j=1}^{2n} q\right)r\right]\prod_{j=1}^{2n} d^2q_j \quad \text{(A3)}$$

will appear with $i^{2n}=(-1)^n$. These integrals for $n=1,2$ can be calculated by using Eqs. (4.2), (4.3), and (A.2). Thus, the integrals in Eq. (A3) for $n=1,2$ will be given by

$$-\int \langle h(q_1)h(q_2)\rangle(q_1q_2)e^{-i(q_1+q_2)r}d^2q_1d^2q_2 = S_r(\sigma,\xi,H), \quad \text{(A4a)}$$

$$\int \left\langle \prod_{j=1}^{4} h(q_j)\right\rangle\left(\prod_{j=1}^{4} q_j\right)\exp\left[-i\left(\sum_{j=1}^{4} q_j\right)r\right]\prod_{j=1}^{4} d^2q_j = 3[s_r(\sigma,\xi,H)]^2. \quad \text{(A4b)}$$

For $n>2$, we obtain

$$i^{2n}\int \left\langle \prod_{j=1}^{2n} h(q_j)\right\rangle\left(\prod_{j=1}^{2n} q_j\right) \times\exp\left[-i\left(\sum_{j=1}^{2n} q_j\right)r\right]\prod_{j=1}^{2n} d^2q_j = P(n)[S_r(\sigma,\xi,H)]^{2n}, \quad \text{(A5)}$$

where further concepts of statistics are needed to calculate $P(n)$, which represents all possible ways to group $2n-h(q)$'s ensemble averaged in pairs of two.[15] In fact, the full expansion in Eq. (3.2) after ensemble average is given by

$$A_x \approx A_{flat} + \sum_{n=1}^{+\infty} \frac{1/2(1/2-1)\cdots(1/2-n+1)}{n!} \times\int \langle(\nabla h)^{2n}\rangle d^2r, \quad \text{(A6)}$$

and after substitution from Eqs. (A5) and (A3) yields

$$A_x \approx A_{flat} + \sum_{n=1}^{+\infty} \frac{1/2(1/2-1)\cdots(1/2-n+1)}{n!}\,P(n) \times[S_r(\sigma,\xi,H)]^n \quad \text{(A7)}$$

with $P(1)=1$ and $P(2)=3$.

[1] E. Becquerel and C. R. Hedb, Seances Acad. Sci. **9**, 561 (1839).
[2] F. Lasnier and T. G. Ang, in *Photovoltaic Engineering Handbook* (IOP, Bristol, 1990). For the general theory on heteojunctions see also S. J. Fonash, J. Appl. Phys. **51**, 2115 (1980).
[3] D. Haynes, ''The Solar Energy Timetable,'' Worldwatch Paper **19** (April 1978).
[4] R. F. Service, Science **269**, 920 (1995).
[5] H. Aperathitis, Gr. Phys. Rev. E **14**, 15 (1987); R. H. Bube *et al.*, IEEE Trans. Electron. Devices **ED-24**, 487 (1977); K. Yamagushi *et al.*, Jpn. J. Appl. Phys. **15**, 1575 (1976); **16**, 1203 (1977); F. G. Courreges *et al.*, *ibid*. **51**, 2175 (1980); G. A. Niklasson and C. G. Cranqvist (private communication). For recent work on various systems see also Solar Alert, *ISES '95 (In Search of the Sun, Conference)* (Elsevier Science, New York, 1995).
[6] P. Meakin, Phys. Rep. **235**, 1991 (1994); J. Krim and G. Palasantzas, Int. J. Mod. Phys. Mod. Phys. B **9**, 599 (1995) (Schematics similar to Fig. 1 in this work which show the effect of H, can also be found in Fig. 1 of this reference).
[7] A. M. Barnett and A. Rothwarf, IEEE Trans. Electron. Devices **ED-27**, 615 (1980).
[8] B. B. Mandelbrodt, *The Fractal Geometry of Nature* (Freeman, New York, 1982); F. Family and T. Viscek, *Dynamics of Fractal Surfaces* (World Scientific, Singapore, 1991). The schematics of Fig. 1 are shown only the effect of the roughness exponent H without including any particular σ and ξ, and can be produced by computer graphic algorithms: see R. F. Voss, in *Fundamental Algorithms for Computer Graphics*, edited by R. A. Earshaw (Springer, Berlin, 1985), p. 808; R. F. Voss, in *Scaling Phenomena in Disordered Systems*, edited by R. Pynn and A. Skjeltrop (Plenum, New York, 1985), p. 1.
[9] G. Palasantzas and J. Krim, Phys. Rev. Lett. **73**, 3564 (1994).
[10] G. Palasantzas, Phys. Rev. E **49**, 1740 (1994); J. Krim and J. O. Indekeu, *ibid*. **48**, 1576 (1993).
[11] G. Palasantzas, Phys. Rev. B **48**, 14472 (1993); **49**, 5785E (1994).
[12] G. Amar *et al.*, Phys. Rev. Lett. **64**, 542 (1990); J. Krug *et al.*, *ibid*. **64**, 2332 (1990); J. M. Kim *et al.*, *ibid*. **64**, 2333 (1990); D. A. Huse *et al.*, Phys. Rev. B **41**, 7075 (1990).
[13] J. Villain *et al.*, J. Phys. F **15**, 805 (1985); J. Jose *et al.*, Phys. Rev. B **16**, 1217 (1977).
[14] G. A. Farias and A. A. Maradudin, Phys. Rev. B **28**, 5675 (1983). See page 5676 for these basic concepts of random rough surfaces.
[15] M. R. Spiegel, in *Probability and Statistics* (Schaum's Outline Series, McGraw-Hill, New York, 1975).